Zhuo *et al.*
European Journal of Medical Research (2024) 29:414
https://doi.org/10.1186/s40001-024-02010-3

European Journal of Medical Research

RESEARCH

Open Access

CYB561 is a potential therapeutic target for breast cancer and is associated with immune cell infiltration

Jian Zhuo[1], Yanchun Zhao[2], Ruiying Hao[3], He Li[3], Zilin Zheng[3], Luxian Dai[1], Ankang Sheng[1], Hanyu Yao[1], Yubao Tang[1], Rao Wang[1], Xiaohong Yang[1] and Weiguang Liu[1*]

Abstract

Background Breast cancer (BC), a common malignant tumor originating from the terminal ductal lobular unit of the breast, poses a substantial health risk to women. Previous studies have associated cytochrome b561 (CYB561) with a poor prognosis in BC; however, its underlying mechanism of this association remains unclear.

Methods We investigated the expression of CYB561 mRNA in BC using databases such as The Cancer Genome Atlas, Gene Expression Omnibus, Tumor–Normal–Metastatic plot, and Kaplan–Meier plotter databases. The prognostic value of CYB561 protein in BC was assessed in relation to its expression levels in tumor tissue samples from 158 patients with BC. The effect of CYB561 on BC progression was confirmed using in vivo and in vitro experiments. The biological functions and related signaling pathways of CYB561 in BC were explored using gene microarray, Innovative Pathway, Gene Ontology enrichment, and Kyoto Encyclopedia of Genes and Genomes enrichment analyses. The correlation between CYB561 and the BC tumor immune microenvironment was evaluated using the CIBERSORT algorithm and single-cell analysis and further validated through immunohistochemistry of serial sections.

Results Our study demonstrated that upregulation of CYB561 expression predicted poor prognosis in patients with BC and that CYB561 knockdown inhibited the proliferation, migration, and invasive ability of BC cells in vitro. CYB561 knockdown inhibited BC tumor formation in vivo.CYB561 was observed to modulate downstream tropomyosin 1 expression. Furthermore, CYB561 expression was associated with macrophage M2 polarization in the BC immune microenvironment.

Conclusions Elevated CYB561 expression suggests a poor prognosis for patients with BC and is associated with macrophage M2 polarization in the BC microenvironment. Therefore, CYB561 could potentially serve as a therapeutic target for BC treatment.

Keywords Cytochrome b561 (CYB561), Breast cancer (BC), Prognosis, Bioinformatics, Immune infiltration, Single-cell sequence

*Correspondence:
Weiguang Liu
lwg1943@163.com
[1] Department of Breast Surgery, Yangzhou Maternal and Child Health Care Hospital Affiliated to Yangzhou University, Yangzhou 225007, Jiangsu, China
[2] Department of Outpatient, Affiliated Hospital of Hebei University of Engineering, Handan 056000, Hebei, China
[3] School of Clinical Medicine, The Hebei University of Engineering, Handan 056000, Hebei, China

Background

Breast cancer (BC) is a common malignant tumor of the terminal ductal lobular unit of the breast that poses a serious health risk to women [1]. In 2020, the global incidence of the disease was 11.7%, with a mortality rate of 30% [2]. The primary causes of death due to this disease include invasive metastases and recurrence [3, 4]. The heterogeneous nature of BC because of its diverse mechanisms of action complicates the selection of appropriate treatments [5]. Notwithstanding the substantial advancements made in understanding the pathogenesis and diagnosis of this disease, there is a dire need to explore new therapeutic approaches, considering its multifactorial nature and the involvement of numerous pathways.

Cytochrome b561 (CYB561), a member of the CYB561 family, contains two transmembrane heme b cytochromes and is genetically located on human chromosome 17q [6]. This protein is ubiquitously expressed in humans and exhibits a variety of biological functions [7]. Diseases are often associated with dysfunction. A deficiency in CYB561 can result in selective failure of the sympathetic noradrenergic system [8], and pathogenic mutations in CYB561 can cause orthostatic hypotension [9]. Besides, aberrant CYB561 expression has been linked to a poor prognosis in endometrial, non-small cell lung, and ovarian cancers [10–12]. Although previous studies have identified CYB561 as a potential marker of poor prognosis in BC through bioinformatics and immunohistochemical analyses [13, 14], the mechanism of CYB561 involvement in BC progression is unclear.

Methods

Bioinformatics analysis using online databases

The mRNA expression of CYB561 in BC was assessed using gene chip data from the Tumor–Normal–Metastatic plot (TNMplot) database (https://tnmplot.com/). The overall survival (OS) and recurrence-free survival (RFS) curves for CYB561 in BC were constructed using the gene chip dataset of the Kaplan–Meier plotter database (http://kmplot.com/).

Data retrieval and analysis

A total of 1,087 TCGA-BRCA samples, including RNA expression data (HTSeq-FPKM) and corresponding clinical information, were downloaded from the TCGA database (https://portal.gdc.cancer.gov/). Similarly, from the Gene Expression Omnibus (GEO) database [15], dataset GSE199515, which included single-cell RNA sequencing (scRNA-seq) of tumor tissue samples from 3 BC cases, was acquired from the GEO database [15]. Datasets GSE65194 and GSE139038, containing 130 and 41 BC mRNA expression profiles, respectively, along with clinical information, were obtained from the GEO database. Differential gene analysis was subsequently conducted using the "limma" package in R. After filtering the HTSeq-FPKM data, the ComBat function in the sva package was used to eliminate inter-batch differences. A box plot was used to visualize the normalization process, and a principal component analysis (PCA) clustering diagram was used to demonstrate the inter-sample correction effect. The debatched data were used in subsequent experiments.

scRNA-seq data quality control

The scRNA-seq data were preprocessed, including normalization and filtering of cells expressing fewer than 300 genes or cells with mitochondrial genes, accounting for over 25% of the total genes. The number of genes detected in a single cell (nFeature) and total number of molecules (nCount) were calculated using Seurat's standard procedure. The PercentageFeatureSet function was used to calculate the ratio of mitochondrial genes (MitoRatio), with the following quality control parameters: $500 \leq n$ Count; $300 \leq n$ Features $\leq 3\,000$; MitoRatios $\leq 1\%$. After quality control, the data were normalized using the Normalize Data function, followed by unique molecular identifier and gene correlation analyses to assess data quality.

scRNA-seq data analysis

The scRNA-seq dataset GSE199515 for BC was obtained from the GEO database and analyzed using the "Seurat" R package. PCA was performed to reduce the dimensionality of the highly variable gene expression profiles. JackStrawPlot and ElbowPlot functions were used to select the principal components for downstream analysis. The clustering results were visualized in two-dimensional space using the UMAP algorithm. Cell annotation within the identified clusters was conducted using the "SingleR" R package. The "monocle2" software package was used for trajectory analysis, followed by the screening of differentially expressed genes within the clustering results, dimensionality reduction using the DDRTree method, and subsequent cell selection and trajectory construction. Heatmaps of selected gene expression were generated following clustering analysis, presenting the expression trends of the top 100 drivers and target genes within each cell cluster.

Clinical correlation analysis

To assess the independent predictive ability of the CBY561 gene-based grouping model for patients with BRCA, we first analyzed the correlation between CYB561 and clinicopathological characteristics of patients with BC via Chi-square test using TCGA dataset. The associated independent prognostic factors were identified using

univariate and multivariate Cox regression analyses. The factors included age, sex, and World Health Organization classification. In addition, the receiver operating characteristic (ROC) curves were constructed and area under the ROC curve (AUC) values were calculated to estimate the predictive performance of the model.

Development and evaluation of column line diagrams

A nomogram was developed to serve as a clinically applicable tool for predicting the prognosis of patients with BRCA at 1-, 3-, and 5-year intervals. A nomogram was constructed based on the results of Cox regression analysis, incorporating prognostic factors such as sex, age, and grade. The discriminative ability of the nomogram was evaluated using calibration plots and was quantified as a consistency index.

Functional enrichment analysis

The "clusterProfiler" package [16] in R was employed for Gene Ontology (GO) and Kyoto Encyclopedia of Genes and Genomes (KEGG) [17] enrichment analyses on 45 key genes, with a significance threshold of $p < 0.05$. GO enrichment analysis included the categories of Biological Processes (BP), Cellular Components (CC), and Molecular Functions (MF). The identifiers for the top 20 terms in each category were selected and visualized using a bubble plot. KEGG enrichment analysis was conducted with a significance threshold of $p < 0.05$. Gene Set Enrichment Analysis was subsequently performed to explore the potential molecular mechanisms between the two stated risk groups. Gene set permutations were set at one, with significant terms meeting the following conditions: false discovery rate < 0.001 and p-value < 0.25.

Analysis of the immune microenvironment

To investigate the immune microenvironment of BRCA, transcriptomic data were used along with the CIBERSORT algorithm to calculate the proportion of 22 immune cell types [18]. The relative proportions of these immune cell types were compared between the two groups based on the median values of CBY561. The correlation between CBY561 expression and immune cells as well as immune checkpoints was also analyzed. Further assessment of the immune infiltrate cell index was conducted using estimation tools.

Human specimens

This study included 158 patients with BC. The inclusion criteria were as follows: (1) patients who underwent BC surgery at the Yangzhou Maternal and Child Health Care Hospital affiliated with Yangzhou University between January 2013 and December 2015. (2) Each patient had a pathological diagnosis of invasive ductal carcinoma of the breast accompanied by comprehensive clinicopathological information. (3) All patients received standard postoperative adjuvant therapy, including chemotherapy, radiotherapy, endocrine therapy, or targeted therapy. (4) All patients had available 5-year postoperative follow-up data. The exclusion criteria were as follows: (1) preoperative neoadjuvant therapy; (2) distant metastases or ineligibility for surgery; (3) concurrent presence of other malignancies; (4) coexistence of severe psychiatric or autoimmune diseases, and (5) age < 18 years. All methods were implemented in accordance with the relevant guidelines and regulations of the Declaration of Helsinki. This study was retrospective in nature and anonymization of all patient information would not have impacted the treatment and therefore approval was obtained from the Ethics Committee of Yangzhou Maternal and Child Health Care Hospital Affiliated to Yangzhou University to waive patient informed consent.

Immunohistochemistry (IHC)

For IHC, paraffin-embedded BC tissue samples were sectioned into 4-μm-thick slices. These were then processed through baking, dewaxing, and dehydration, followed by the elimination of endogenous peroxidase activity using a 3% H_2O_2 solution and antigen repair with 0.01 mol/L citrate buffer. The sections were blocked with 3% goat serum, followed by the addition of CYB561 primary antibody (1:100) and incubation at 4 °C overnight. The secondary antibody was then added and incubated at 37 °C for 20 min, followed by 3,3′-diaminobenzidinecolor development, hematoxylin re-staining, and neutral gum sealing. The expression of CYB561 in the BC tissues was assessed by two senior pathologists. CYB561 protein expression was analyzed using the Immunoreactive Score system, and "score ≤ 3" was regarded as CYB561 negative expression, and "score > 3" was regarded as CYB561 positive expression.

BC cell lines

The BC cell lines, MCF-7, MDA-MB-361, SK-BR-3, HCC1937, and MDA-MB-231, were procured from the American Type Culture Collection (USA). These BC cells were cultured in RPMI-1640 medium, supplemented with 100 U/mL penicillin, 0.1 mg/mL streptomycin, and 10% fetal bovine serum (FBS), under conditions of 37 °C and 5% CO_2.

RNA interference

For RNA interference, recombinant lentiviruses encoding short hairpin RNAs (shRNAs) specific to human CYB561 were designed and prepared by GeneChem (Shanghai, China). The CYB561 target sequences used were as follows: CYB561-shRNA#1, 5′-CGCCCACAGCACATC

TTCTTT-3′; CYB561-shRNA#2, 5′-GCACATCTTTGC GCTCGTCAT-3′; CYB561-shRNA#3, 5′-CCTGCTGGT TTACCGTGTCTT-3′. A scrambled (scr)-shRNA was used as a negative control, with the target sequence being 5′-TTCTCCGAACGTGTCACGTTT-3′. The lentivirus was added to the cells according to the manufacturer's instructions. The CYB561 knockout rate was quantified using quantitative real-time PCR (qRT-PCR) and western blotting.

RNA extraction and qRT-PCR

RNA was extracted using TRIzol reagent according to the manufacturer's instructions (Invitrogen). The expression levels of CYB561 were determined using qRT-PCR. The primers used for CYB561 were: forward, TATAGCGCA TTTGAGCCCGAG and reverse, CCGGGTCAAGAT GTAGAGCAC. The internal reference GAPDH primers were as follows: forward, TGACTTCAACAGCGACAC CCA and reverse, CACCCTGTTGCTGTAGCCAAA.

Western blotting

For western blotting, BC cells were collected and lysed on ice for 30 min in a lysis solution containing 20 mM Tris–HCl (pH 7.4), 150 mM NaCl, 1% Triton x-100, and protease inhibitors. The supernatant was collected via centrifugation at 12,000 rpm for 10 min at 4 °C with a 10-cm radius. The total protein concentration was determined using a bicinchoninic acid, protein assay kit (Pierce). Nitrocellulose membranes were cut and blocked with 5% skim milk (diluted in 1×phosphate-buffered saline [PBS]) for 2 h at room temperature. Subsequently, the CYB561 antibody (1:1000, Invitrogen, PA5-53228) and α-tubulin (1:10,000, Proteintech, 11224-1-AP) was added and incubated overnight at 4 °C. The membrane was then washed with 1×PBS for 50 min, followed by the addition of the secondary antibody for 40 min at room temperature. After washing for 20 min, enhanced chemiluminescence (Amersham) was used to visualize the proteins in a dark chamber. After 5 min at room temperature, the membranes were exposed and developed.

Clone formation assay

In the clone formation assay, lentivirus-infected cells carrying CYB561-shRNA or scr-shRNA were collected via trypsin digestion and mixed with medium containing 10% FBS to form a single-cell suspension of ~ 1×10^4 cells/mL. An appropriate amount of the cell suspension was inoculated into a 6-well plate; ~ 500 cells were inoculated per well, 6 mL of culture medium containing 10% FBS was added, and the solution was changed every 3 days. The culture was terminated when clonal clusters formed on the 6-well plate, as seen by the naked eye, or when the number of cells in most of the individual clones was greater than 50, as observed under the microscope. The plates were fixed with 4% paraformaldehyde for 30 min, the fixative was removed, and the cells were stained with a crystal violet staining solution for 30 min, washed, dried, photographed, and counted.

MTT assay

In the MTT assay, lentivirus-infected cells carrying CYB561-shRNA or scr-shRNA were collected by trypsin digestion and mixed with a medium containing 10% FBS to form a single-cell suspension of ~ 1×10^4 cells/mL. The cell suspension was then plated in 96-well plates (100 μL/well). After 12–72 h of incubation, 10 μl MTT (5 mg/ml) was added to each well. The culture was terminated after 4 h and the culture supernatant was carefully removed from the wells. For the cell suspension, the culture supernatant was removed after centrifugation, 100 μl DMSO was added to each well, and the absorbance was measured at 490 nm using an enzyme marker. Each group was analyzed in triplicates.

Wound healing assay

For the wound healing assay, the collected BC cells were inoculated into a 24-well plate and cultured. After the cells had adhered, a scratch was made using a 1-mL pipette tip, and the residual cells were washed with PBS. The cells were then cultured in RPMI-1640 containing 10% FBS, and wound healing was examined after 24 h using a microscope and photographed for analysis.

Transwell assay

For the transwell assay, the transwell chambers, consisting of 24-well tissue culture plates and 12-well cell culture inserts with polycarbonate membranes of 8 μm pore size, were used. Serum-free cell suspensions were prepared and counted at a density of 1×10^6 cells/well (24-well plates). Serum-free cell suspension (100 μL/well) was added to the upper chamber and 600 μL of RPMI-1640 medium containing 30% FBS was added to the lower chamber. The cells were incubated at 37 °C for 16 h, then fixed with 4% paraformaldehyde for 30 min, stained with 0.5% crystal violet stain, and transferred to the lower surface of the membrane for 1–3 min. The images were captured under a microscope at 200 × magnification for cell counting and analysis.

Tumor growth in nude mice

Female BALB/c nude mice (4–6 weeks old) were purchased from Shanghai Lingchang Biotechnology Co. MDA-MB-231 cells (1×10^7) transfected with CYB561-shRNA or scr-shRNA were subcutaneously implanted into the right anterior scapula of female BALB/c nude mice.

After 7 weeks, the nude mice were injected with an overdose of 2% pentobarbital sodium, killed, and the tumors were weighed. Animal handling and study protocols were approved by the Ethics Committee of the Yangzhou Maternal and Child Health Care Hospital, affiliated with Yangzhou University.

Microarray detection and data analysis

For microarray detection and data analysis, total RNA was isolated from MDA-MB-231 cells using the TRIzol reagent. The cells were then transfected with lentiviral vectors carrying either scr-shRNA or CYB561-shRNA. The RNA samples were quantitatively assessed using a NanoDrop 2000 spectrophotometer and an Agilent 2100 system. Following the synthesis of complementary DNA strands via reverse transcription, labeled complementary RNA (cRNA) molecules were enzymatically generated through in vitro transcription using a GeneChip 3IVT Expression Kit. The cRNA samples were then hybridized using the GeneChip Hybridization Wash and Stain Kit, which included sequential phases of hybridization, washing, and staining. Data were acquired using the GeneChip Scanner 3000 software. The resulting dataset was used to investigate gene expression profiles on the Affymetrix Human Gene 1.0 ST platform. Genes with differential expression between MDA-MB-231 cells hosting CYB561-shRNA and scr-shRNAs were identified based on criteria set at $p < 0.05$ and $|FC| > 1.5$, indicating statistical and magnitude-based significance, respectively. An Innovative Pathway Analysis (IPA) database was used for pathway analyses, disease-related investigations, functional annotations, network analyses, and downstream genetic inquiries.

Statistical analysis

In the statistical analysis, non-paired *t*-tests were used for comparisons between two groups, while one-way analysis of variance (ANOVA) was used for comparisons involving more than two groups. Variables analyzed at different time points were assessed using repeated-measures ANOVA. The Wilcoxon signed-rank test was used to compare ordinal data in the clinical cohort datasets, whereas the Chi-square test ($\chi 2$ test) was used to compare between-group data. All statistical analyses were performed using SPSS 22.0 software and GraphPad Prism 8.0. Statistical significance was set at $p < 0.05$. The symbols used to denote significance levels are as follows: * indicates p less than 0.05, ** indicates $p < 0.01$, and *** indicates $p < 0.001$. Measurement data are presented as mean ± standard deviation.

Results

Elevated expression of CYB561 mRNA is indicative of a poor prognosis in BC

Pan-cancer analysis utilizing the TNM plot database revealed increased expression of CYB561 mRNA across various tumors. Moreover, gene microarray data, comprising 7569 BC and 242 normal breast cases, demonstrated significant upregulation of CYB561 mRNA in BC ($p < 0.001$, Fig. 1A). The relationship between CYB561 mRNA and clinical parameters such as age, sex, grade, T, N, M, and TNM stage in patients with BC was subsequently analyzed using TCGA database (Fig. 1B). The CYB561 mRNA expression levels of 1087 BC patients from TCGA database were categorized into high and low expression groups. An analysis of these groups, in conjunction with their clinical characteristics, revealed a correlation between CYB561 mRNA expression levels and age, menopausal status, and OS in BC patients ($p < 0.05$, Table 1). ROC curves, constructed from the GEO database datasets GSE139038 and GSE15852, demonstrated the diagnostic significance of CYB561 for BC, with AUC1 = 0.930 (95% confidence interval [CI] 0.879–0.971) and AUC2 = 0.932 (95% CI 0.868–0.981) (Fig. 1C).

Survival curves constructed based on the Kaplan–Meier plotter database indicated that patients with BC with high CYB561 mRNA expression had worse OS ($p < 0.05$) and RFS ($p < 0.05$, Fig. 1D). Utilizing the sample data of patients with BC from TCGA database, CYB561 was incorporated with clinical characteristics for univariate and multivariate Cox regression analyses. CYB561 was identified as an independent risk factor for BC (Fig. 1E). Subsequently, a nomogram was constructed as a clinical prediction model to estimate the 1-, 3-, and 5-year survival probabilities of patients (Fig. 1F). The nomogram had a C-index of 0.838 and predicted AUCs of 0.992, 0.954, and 0.912 for 1-, 3-, and 5-year OS, respectively. The calibration plots demonstrated good

(See figure on next page.)

Fig. 1 Expression and clinical characterization of CYB561 mRNA in BC. **A** Pan-cancer analysis of CYB561 mRNA expression levels based on the TNMplot database. **B** Correlation between CYB561 mRNA expression level and BC patients age, sex, grade, T, N, M, WHO stage based on TCGA database. **C** ROC curve analysis of the diagnostic performance of CYB561 gene in two datasets GSE65194 and GSE139038. **D** Construction of OS, RFS survival curves of CYB561 mRNA and BC patients based on Kaplan–Meier Plotter database. **E** Based on the TCGA database, univariate and multivariate Cox regression analyses were performed to analyze CYB561 mRNA as an independent risk factor for BC. **F** Construction of a clinical model nomogram based on TCGA multifactor Cox regression analysis

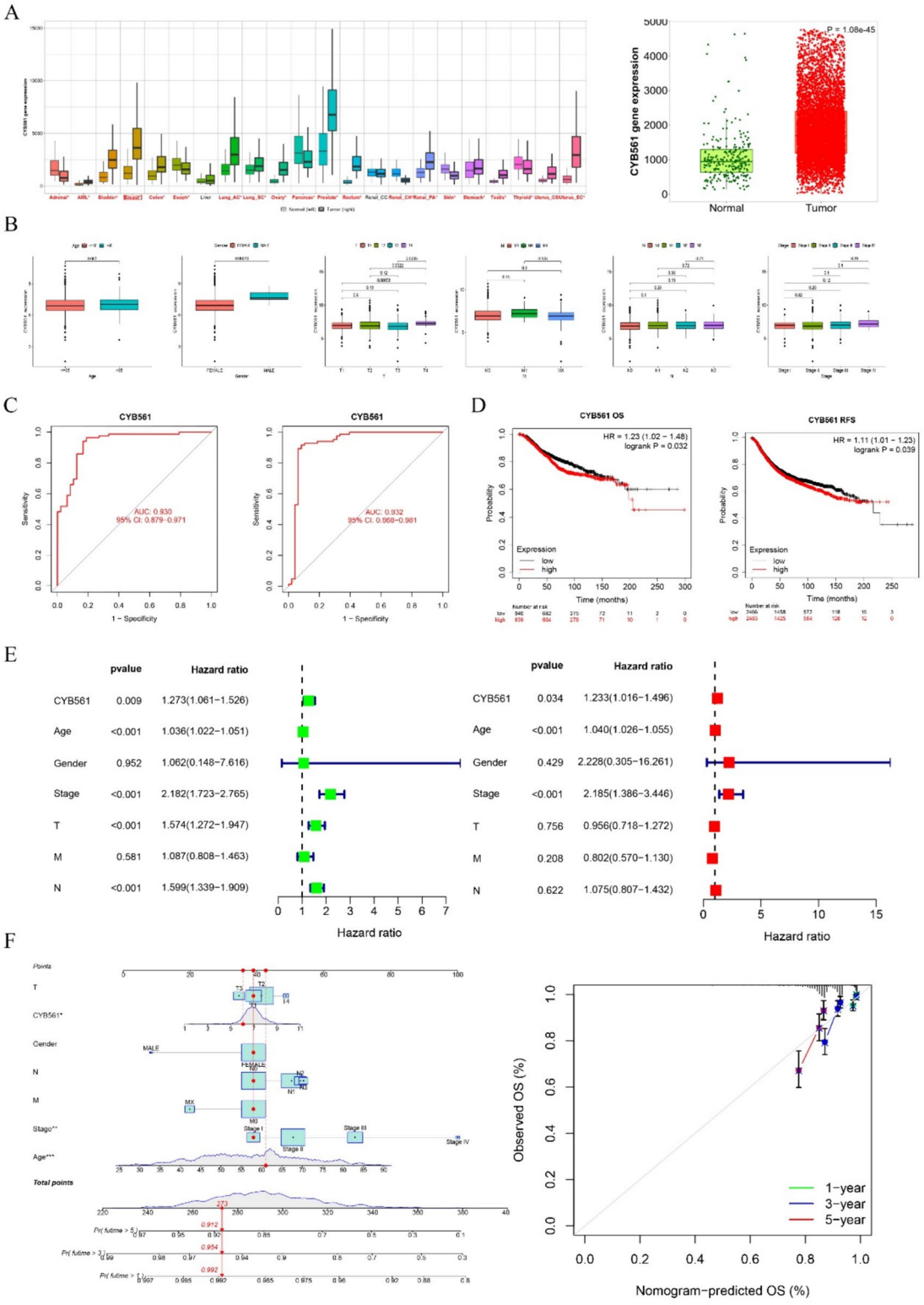

Fig. 1 (See legend on previous page.)

Table 1 Correlation analysis between CYB561 mRNA expression level and clinical characteristics ($N = 1087$)

Characteristics	CYB561 mRNA expression level		*p* value	χ^2
	Low expression	High expression		
N	543	544		
Age, *n* (%)			0.011	6.431
≤ 60	322 (29.6%)	281 (25.9%)		
> 60	221 (20.3%)	263 (24.2%)		
Menopause status, *n* (%)			0.001	14.506
Pre	129 (13.2%)	101 (10.3%)		
Peri	29 (3%)	11 (1.1%)		
Post	330 (33.8%)	376 (38.5%)		
Anatomic neoplasm subdivisions, *n* (%)			0.975	0.001
Left	283 (26%)	283 (26%)		
Right	260 (23.9%)	261 (24%)		
Pathologic T stage, *n* (%)			0.783	0.490
T1	134 (12.4%)	144 (13.3%)		
T2	320 (29.5%)	311 (28.7%)		
T3 and T4	87 (8%)	88 (8.1%)		
Pathologic N stage, *n* (%)			0.679	1.514
N0	268 (25.1%)	248 (23.2%)		
N1	176 (16.5%)	183 (17.1%)		
N2	58 (5.4%)	58 (5.4%)		
N3	35 (3.3%)	42 (3.9%)		
Pathologic M stage, *n* (%)			0.669	0.183
M0	451 (48.8%)	454 (49.1%)		
M1	9 (1%)	11 (1.2%)		
Pathologic stage, *n* (%)			0.330	3.433
Stage I	84 (7.9%)	98 (9.2%)		
Stage II	325 (30.6%)	294 (27.7%)		
Stage III	116 (10.9%)	128 (12%)		
Stage IV	8 (0.8%)	10 (0.9%)		
OS event, *n* (%)			0.024	5.115
Alive	480 (44.2%)	455 (41.9%)		
Dead	63 (5.8%)	89 (8.2%)		

agreement between the predicted and observed 1-, 3-, and 5-year survival rates.

Expression and prognostic value of CYB561 protein in BC

Immunohistochemical staining was conducted on tumor tissue samples from 158 patients with BC to evaluate CYB561 protein expression. The findings revealed a positive expression rate of 48.1% for CYB561 protein in BC (Fig. 2A). A Chi-square test integrating pathological characteristics and CYB561 protein expression demonstrated an association between CYB561 protein expression and BC grade, subtype, ER status, PR status, and HER2 status ($p < 0.05$, Table 2). To further investigate the correlation between the expression level of CYB561 protein and pathological characteristics of patients with BC, one-way logistic regression analysis revealed a positive correlation between CYB561 protein expression level and HR-/HER2 + and triple-negative breast cancer (TNBC) subtypes, whereas a negative correlation was observed between ER and PR status ($p < 0.05$,Table 3). Kaplan–Meier survival curves were constructed using follow-up information from the clinical cohort, revealing that patients with BC with positive CYB561 protein expression had poorer 5-year OS ($p < 0.05$, Fig. 2B) and RFS ($p < 0.05$, Fig. 2C). Univariate Cox regression analysis identified age, Grading, pTNM stage, T stage, N stage, and CYB561 status as risk factors for RFS, with ER and PR status as protective factors. In terms of OS, pTNM stage, T stage, N stage,

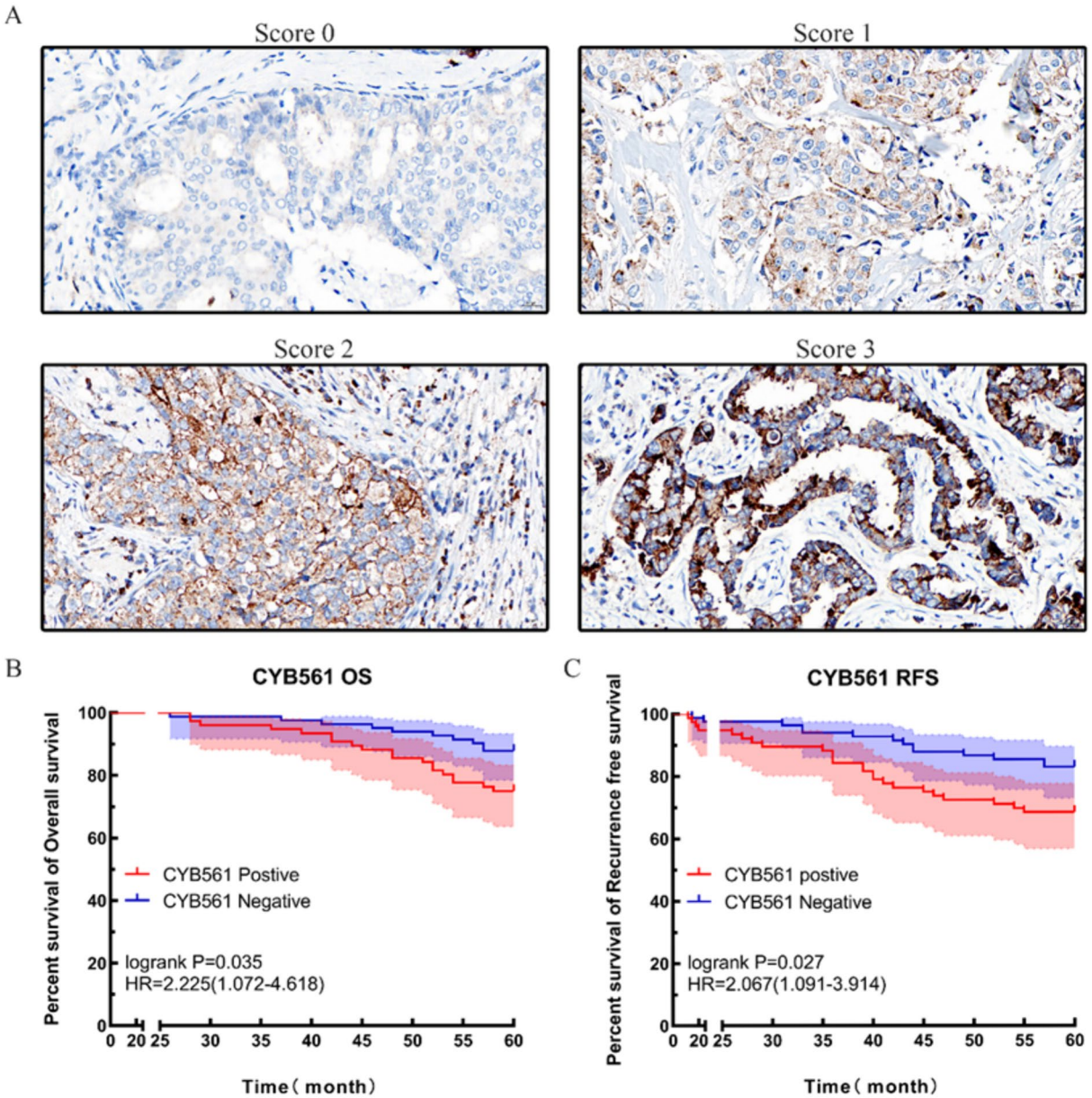

Fig. 2 CYB561 protein expression in BC and clinical prognosis. **A** CYB561 protein is expressed at different levels in BC tissues (Magnification 400×). **B** CYB561 protein and OS survival curves in BC patients. **C** CYB561 protein and RFS survival curves in BC patients

subtype, and CYB561 status were risk factors, whereas ER and PR status were protective factors (Table 4).

Correlation of CYB561 with immune cell infiltration

The two cohorts were classified into high- and low-expression groups based on the median CYB561 expression levels. Analysis of immune cell infiltration between these two groups revealed that giant cell M2 was significantly more abundant in the CYB561 high-expression group, while $CD8^+$ T cell was more abundant in the CYB561 low-expression group than their respective counterparts (Fig. 3A). Further analysis of the relationship between CYB561 and BC immune-infiltrating cells indicated a positive correlation with M2 macrophages and a negative correlation with $CD8^+$ T cell levels (Fig. 3B). Immunohistochemical staining of BC samples from the clinical cohort was performed to assess the expression levels of CD8 and the macrophage M2 marker CD163 in tumor-infiltrating lymphocytes (Fig. 3D). The mean CD8 per 400×field of view was 29.39 (range:

Table 2 Chi-square test analysis of CYB561 protein expression level and clinical characteristics ($N=158$)

Characteristics	CYB561 protein expression level		*p* value	χ^2
	Negative expression	Positive expression		
N	82 (51.9%)	76 (48.1%)		
Age, *n* (%)			0.523	0.408
≤60	65 (41.1%)	57 (36.1%)		
>60	17 (10.8%)	19 (12.0%)		
Grading, *n* (%)			0.002	12.909
Grade1	5 (3.2%)	8 (5.1%)		
Grade2	47 (29.7%)	22 (13.9%)		
Grade3	30 (19.0%)	46 (29.1%)		
T stage, *n* (%)			0.299	3.673
T1	39 (26%)	32 (20.3%)		
T2	41 (23.9%)	37 (23.4%)		
T3	1 (0.6%)	5 (3.2%)		
T4	1 (0.6%)	2 (1.3%)		
N stage, *n* (%)			0.578	1.972
N0	48 (30.4%)	45 (28.5%)		
N1	19 (12.0%)	21 (13.3%)		
N2	11 (7.0%)	9 (5.7%)		
N3	4 (2.5%)	1 (0.6%)		
pTNM stage, *n* (%)			0.774	0.513
Stage I	29 (18.4%)	23 (14.6%)		
Stage II	38 (24.1%)	39 (24.7%)		
Stage III	15 (9.5%)	14 (8.9%)		
Subtypes, *n* (%)			0.013	10.854
HR+/HER2−	37 (23.4%)	17 (10.8%)		
HR+/HER2+	21 (13.3%)	21 (13.3%)		
HR−/HER2+	11 (7.0%)	21 (13.3%)		
TNBC	13 (8.2%)	17 (10.8%)		
ER status			0.012	6.264
Negative	25 (15.8%)	38 (24.1%)		
Positive	57 (36.1%)	38 (24.1%)		
PR status			0.004	8.097
Negative	30 (19.0%)	45 (28.5%)		
Positive	52 (32.9%)	31 (19.6%)		
HER2 status			0.041	4.177
Negative	50 (36.1%)	34 (21.5%)		
Positive	32 (20.3%)	42 (26.6%)		

1–114), and the mean CD163 was 33.28 (range: 4–96). Spearman correlation analysis revealed a negative correlation between CYB561 expression and CD8 ($r=-0.166$, $p=0.037$), and a positive correlation with CD163 expression ($r=0.212$, $p=0.007$).

CYB561 expression in BC was examined via single-cell analysis and cellular

The GSE199515 dataset was extracted, and the top 2,000 variable genes were analyzed (Supplementary Fig. 1A). The top 15 principal components were selected for further analysis (Supplementary Fig. 1B), resulting in the grouping of cells into 10 distinct clusters (Supplementary Fig. 1C). Based on the marker genes, these 10 clusters were consolidated into four cell populations: epithelial cells, macrophages, T cells, and B cells (Fig. 4A). The CYB561 gene was predominantly expressed in the epithelial cells and macrophages (Fig. 4B). The expression profiling data were projected onto a low-dimensional space to construct differentiation trajectories between cells.

Table 3 One-way logistic regression analysis of CYB561 protein expression level and clinical characteristics ($N=158$)

Clinicopathologic characteristics	*B*	*p*	HR	95%CI
Grading		0.002		
2	− 1.229	0.050	0.293	0.086–0.998
3	− 0.043	0.410	0.958	0.286–3.208
Subtype		0.015		
HR+/HER2+	0.788	0.068	2.176	0.945–5.012
HR−/HER2+	1.424	0.003	4.155	1.642–10.514
TNBC	1.046	0.026	2.846	1.131–7.161
ER status	− 0.824	0.013	0.439	0.229–0.841
PR status	− 0.923	0.005	0.397	0.209–0.755
HER2 status	0.658	0.042	1.930	1.024–3.637

Two branching points were identified in the differentiation trajectory that represent potential decision points in the cell biology process. By analyzing cell trajectories, we observed that epithelial cells and macrophages were at different stages and that changes in CYB561 expression occurred mainly in the epithelial and macrophage trajectories (Fig. 4C). Subsequently, the biological functions of macrophages in BC were explored via GO enrichment analysis, and the results showed that in addition to immune-related functions, there was a notable association between macrophages and actin filaments (Fig. 4D).

Knockdown of CYB561 in vitro inhibits the proliferation, invasion, and migration ability of BC cells

In this study, we initially assessed CYB561 mRNA expression levels in five BC cell lines, MCF-7, MDA-MB-361, SK-BR-3, HCC1937, and MDA-MB-231, using qRT-PCR (Fig. 5A).

The efficiency of CYB561 mRNA knockdown in vitro was detected using qRT-PCR, and the results showed that the CYB561-shRNA#2 sequence had good knockdown efficiency (Fig. 5B); subsequent experiments were performed using this sequence. Western blotting showed that CYB561-shRNA knocked down the expression of CYB561 in BC cell lines (Fig. 5C). The clone formation assay showed that the in vitro knockdown of CYB561 inhibited the proliferation and tumorigenicity of BC cells (Fig. 5D). The MTT assay showed that in vitro knockdown of CYB561 inhibited the proliferation of BC cells (Fig. 5E). Transwell assays showed that the in vitro knockdown of CYB561 inhibited the invasive ability of

Table 4 Univariate Cox regression analysis of RFS, OS and clinicopathological characteristics of CYB561 ($N=158$)

Factor	Recurrence free survival				Overall survival			
	B	*p*	HR	95%CI	*B*	*p*	HR	95%CI
Age	0.774	0.021	2.169	1.122–4.194	0.652	0.095	1.919	0.892–4.128
Grading		0.647				0.657		
2	0.428	0.568	1.534	0.353–6.672	0.055	0.943	1.056	0.234–4.766
3	0.621	0.403	1.860	0.435–7.958	0.387	0.606	1.473	0.339–6.407
PTNM stage		0.001				0.003		
II	1.362	0.013	3.905	1.340–11.380	1.275	0.044	3.578	1.036–12.361
III	2.040	< 0.001	7.692	2.506–23.612	2.126	0.001	8.378	2.336–30.052
T stage		< 0.001				< 0.001		
T2	0.525	0.162	1.691	0.810–3.529	0.165	0.696	1.179	0.517–2.688
T3	1.973	0.001	7.194	2.287–22.625	1.773	0.007	5.886	1.617–21.434
T4	3.635	< 0.001	37.894	9.726–147.639	3.933	< 0.001	51.085	12.177–214.311
N stage		< 0.001				0.012		
N1	1.295	0.001	3.652	1.727–7.723	0.879	0.044	2.408	1.022–5.672
N2	0.959	0.055	2.609	0.979–6.954	0.849	0.116	2.337	0.812–6.727
N3	2.284	< 0.001	9.813	3.144–30.624	2.015	0.002	7.499	2.087–26.938
Subtype		0.055				0.031		
HR+/HER2+	0.699	0.156	2.013	0.766–5.289	1.298	0.055	3.662	0.971–13.805
HR−/HER2+	1.073	0.030	2.924	1.113–7.686	1.775	0.008	5.900	1.597–21.800
TNBC	1.259	0.009	3.521	1.364–9.087	1.859	0.005	6.416	1.736–23.712
ER status	− 0.783	0.016	0.457	0.241–0.866	− 1.033	0.007	0.356	0.168–0.754
PR status	− 0.777	0.021	0.460	0.238–0.889	− 1.010	0.012	0.364	0.166–0.800
HER2 status	0.293	0.367	1.340	0.709–2.534	0.519	0.169	1.680	0.803–3.519
CYB561 status	0.722	0.031	2.068	1.070–4.000	0.800	0.041	2.226	1.035–4.789

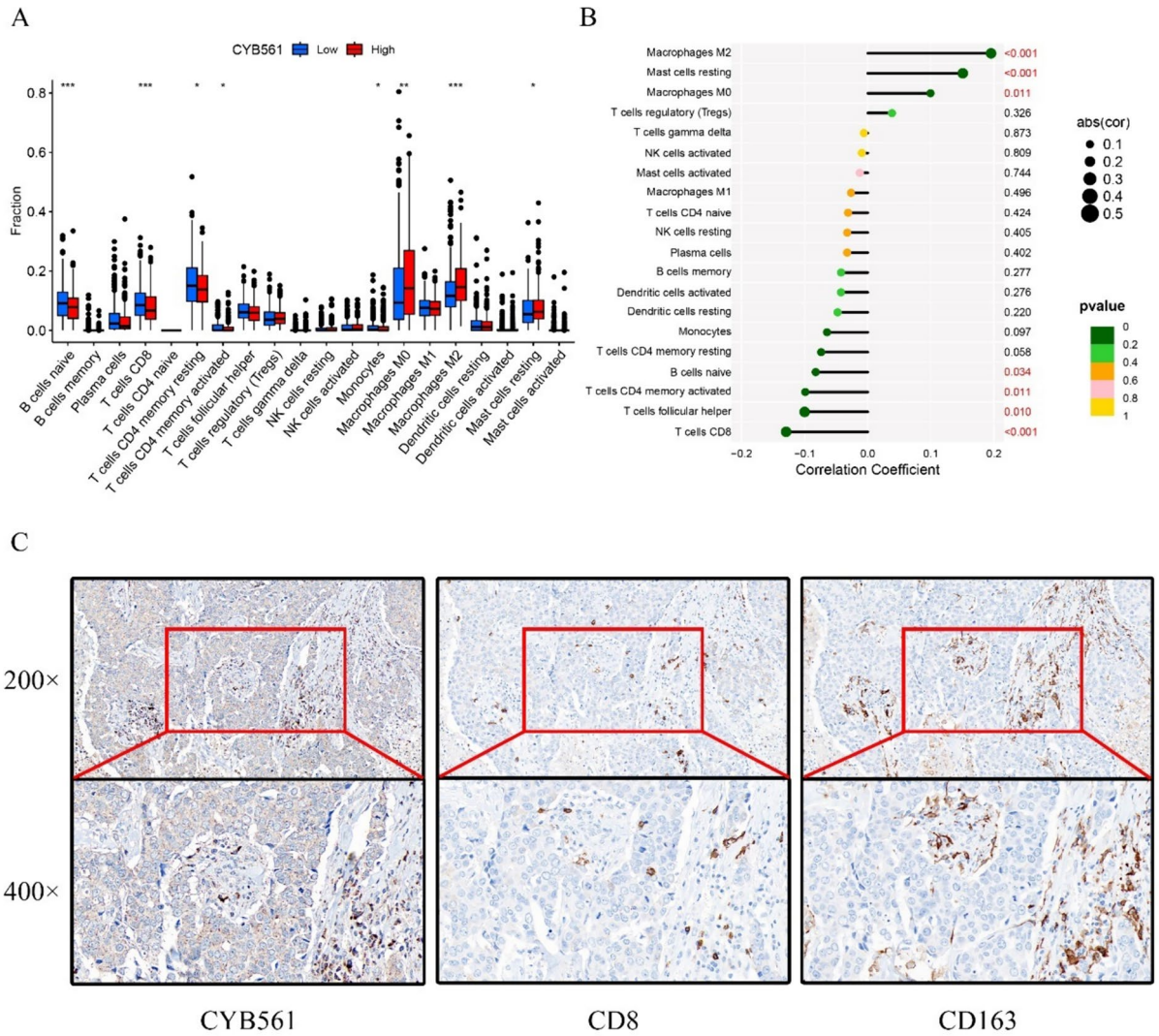

Fig. 3 CYB561 and BC immune cell infiltration. **A** Differences between high and low CYB561 expression subgroups and BC immune infiltrated cells. **B** Correlation of CYB561 with BC tumor-infiltrating immune cells. **C** Immunohistochemical staining of serial sections to assess the expression levels of CYB561, CD8, CD163 in BC (magnification 200×, 400×)

BC cells (Fig. 5F). Furthermore, wound healing assays showed that the in vitro knockdown of CYB561 inhibited the migratory ability of BC cells (Fig. 5G).

CYB561 knockdown inhibits tumor growth in vivo

MDA-MB-231 cells expressing scr-shRNA or CYB561-shRNA were injected subcutaneously into the right anterior scapula of nude mice, and four nude mice were set up in each group. Tumor progression was monitored on a weekly basis until the endpoint of the experiment. The entire study spanned 47 days, during which the tumor volume in the CYB561-shRNA group was found to be significantly smaller than that in the scr-shRNA group ($p < 0.05$, Fig. 6A, B). At the end of the experiment, the tumors in the CYB561-shRNA group weighed significantly less than those in the scr-shRNA group ($p < 0.05$, Fig. 6C).

CYB561-related signaling pathway analysis

The grouping of cells was conducted based on the median CYB561 expression in TCGA database, and relevant differential genes were identified (Supplementary Fig. 2A). Subsequent GO enrichment analyses revealed that CYB561 primarily participates in biological processes, such as immunoglobulin production, humoral immune response, and cytokine activity (Fig. 7A). KEGG enrichment analysis demonstrated that CYB561 interacts with pathways such as cytokine–cytokine receptor

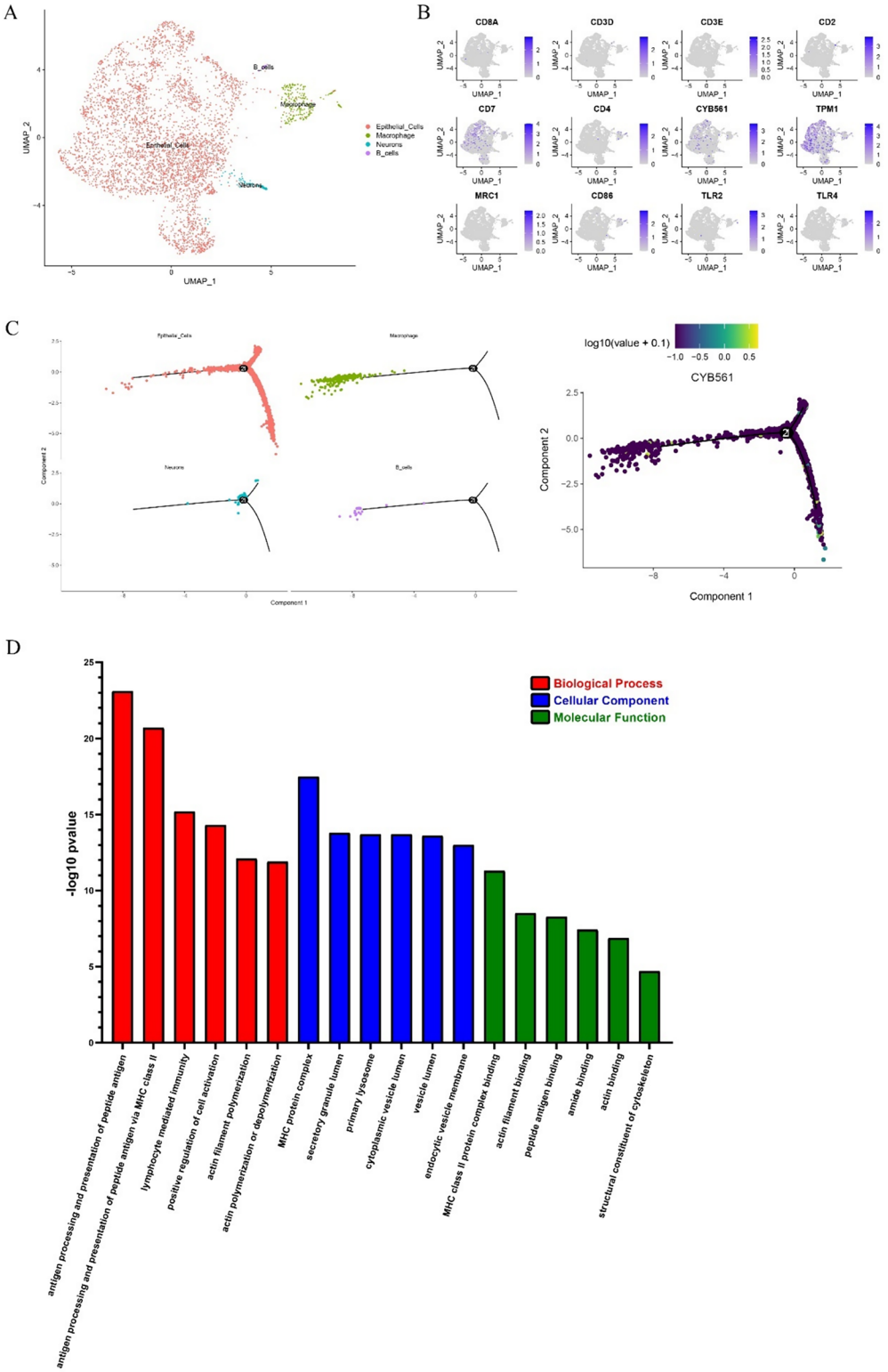

Fig. 4 CYB561 and BC single-cell analysis. **A** Classification and annotation of single-cell subpopulations. **B** Single-cell analysis of CYB561 expression distribution. **C** Proposed time-series analysis of the trajectories of various cell subpopulations and CYB561. **D** GO enrichment analysis explores macrophage-related biological functions

interaction, neuroactive ligand–receptor interaction, and the calcium signaling pathway (Fig. 7B).

We generated gene chip matrices for the MDA-MB-231 cell line CYB561-shRNA and scr-shRNA groups, revealing 287 upregulated and 558 downregulated genes (Supplementary Fig. 2B). The IPA indicated that the biological function of CYB561 was associated with cancer (Fig. 7C). Additionally, IPA highlighted significant enrichment of the calcium signaling pathway, with TPM1 exhibiting significant changes (Fig. 7D).

Next, we constructed an interaction network between CYB561 and TPM1 based on GeneChip data (Fig. 7E). We examined the expression levels of TPM1 and TNNT1 in the reciprocal network using qRT-PCR. The results indicated that TPM1 was significantly upregulated, whereas TNNT1 was downregulated in the CYB561-shRNA group (Fig. 7F).

Discussion

In this study, we initially analyzed the significant upregulation of CYB561 mRNA in BC using an online database and subsequently demonstrated that CYB561 mRNA could potentially serve as a biomarker for BC by constructing a survival curve. To validate the reliability of this conclusion, we performed univariate and multivariate Cox regression analyses by integrating the clinical information of patients in the database. The results indicated that CYB561 is an independent risk factor for BC. Concurrently, the clinical model constructed using the nomogram exhibited a robust predictive performance.

Recognizing that cohorts in online databases may not fully represent real-world clinical cohorts and considering the potential discrepancies between CYB561 mRNA levels and protein expression, we incorporated 158 clinical cohort samples for this retrospective study.

Our results identified a link between CYB561 expression and ER, PR, and HER2 status. Considering the limitations of the Chi-square test analysis, it was further explored using logistic regression, and the results of the analysis demonstrated a positive association between CYB561 expression and BC subtypes HR-/HER2 and TNBC subtypes. Although previous studies [14] have identified a correlation between CYB561 protein expression and HER2, our study uniquely found an association between CYB561 protein expression and TNBC.

HER2-positive TNBC tumors, characterized by high genomic instability and tumor mutation burden, exhibit high levels of immune infiltration [19]. In our transcriptomic analysis, we observed a positive correlation between CYB561 expression and M2 macrophages and a negative correlation with $CD8^+$ T cells. This finding was further corroborated via a single-cell analysis. Serial immunohistochemical sections confirmed that CYB561 positively correlated with CD163 and negatively correlated with $CD8^+$ T cells in the BC immune microenvironment.

Tumor-associated macrophages (TAMs), which are crucial immune cells in the tumor microenvironment, can be classified into classically activated (M1) and alternatively activated (M2) types [20]. CD163, a hemoglobin scavenger receptor, is a marker of M2 type TAM-specific proteins [21]. An increase in CD163 + M2 macrophages predicts the potential for tumor progression through angiogenesis, tissue remodeling, and adaptive immunosuppression, all of which are associated with poor prognostic factors such as early recurrence [22, 23]. CD8 + T cells can act as effector cells against tumor cells, and their accumulation in tumor immune infiltrates is associated with good prognosis [24, 25]. Therefore, we hypothesized that the promotion of BC progression by CYB561 might be related to tumor-infiltrating lymphocytes.

We also examined the expression levels of CYB561 in five BC cell lines and observed the highest CYB561 expression in two triple-negative BC cell lines, HCC1937 and MDA-MB-231. Subsequent cell function and nude mouse tumor formation experiments indicated that CYB561 promoted BC proliferation and invasion both in vivo and in vitro. To further investigate the pro-carcinogenic mechanism of CYB561 in BC, we performed GO and KEGG analyses and GeneChip IPA. Both KEGG analysis and IPA showed significant enrichment in the calcium signaling pathway, where TPM1 levels were negatively correlated with CYB561 expression.

TPM, a double-chain α-helical coiled-coil actin-binding protein, is widely expressed in muscle and non-muscle cells and participates in biological processes such as cytoplasmic division, cell motility, apoptosis,

(See figure on next page.)

Fig. 5 Knockdown of CYB561 in vitro inhibits the proliferation, invasion, and migration ability of BC cells. **A** Expression levels of CYB561 mRNA in BC cell lines. **B** Efficiency of CYB561-shRNA knockdown in BC cells detected by qRT-PCR. **C** Western blot detection of CYB561-shRNA knockdown efficiency in BC cells. **D** Clone formation assay for detection of proliferation and tumorigenicity of BC cells in scr-shRNA and CYB561-shRNA groups. **E** MTT for detection of proliferative capacity of BC cells in scr-shRNA group and CYB561-shRNA group. **F** Transwell assay for BC cell invasion ability in scr-shRNA group and CYB561-shRNA group. **G** Wound healing assays were performed to detect the BC cell migration ability in the scr-shRNA group and the CYB561-shRNA group

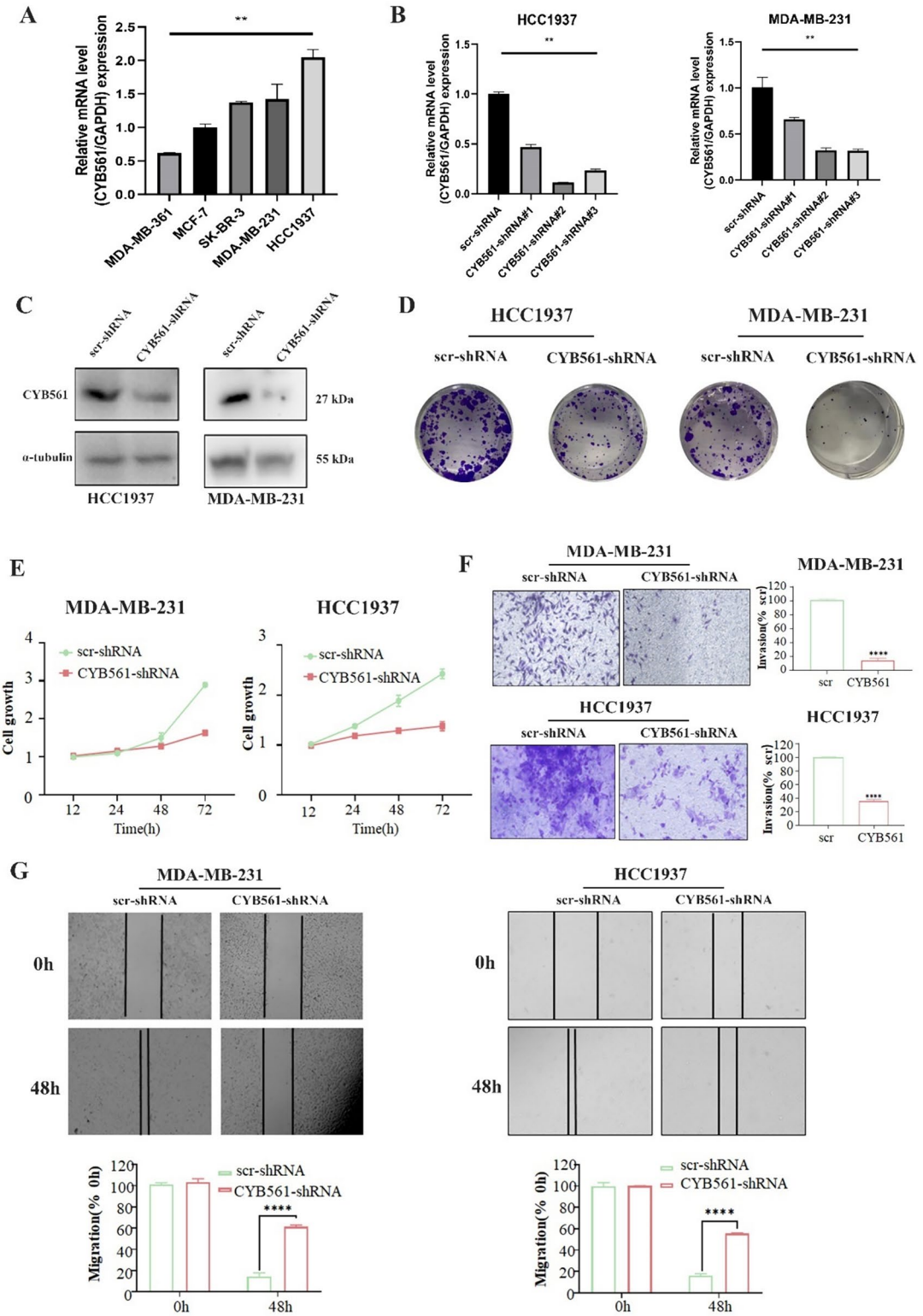

Fig. 5 (See legend on previous page.)

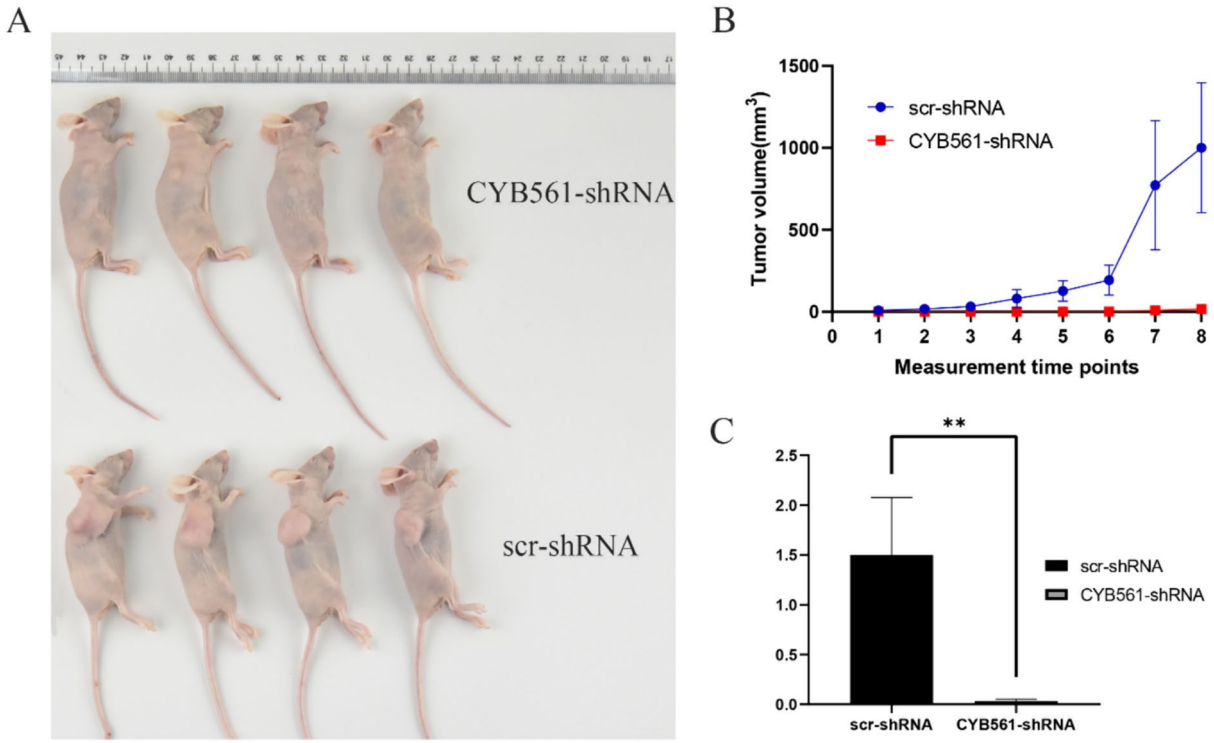

Fig. 6 CYB561 knockdown inhibits tumor growth in vivo. **A** BC cells in the scr-shRNA group and CYB561-shRNA group were tumorigenic in vitro. **B** Volume of BC cells tumorigenic in vitro in the scr-shRNA and CYB561-shRNA groups. **C** Weight of BC cells tumorigenic in vitro in the scr-shRNA and CYB561-shRNA groups

and signaling [26, 27]. TPM1 is considered a tumor suppressor, and its overexpression induces apoptosis in cancer cells during cancer progression [28]. Previous studies have shown that TPM1 expression is much higher in normal breast tissues than in BC tissues, and its increased expression reduces the malignant transformation of breast epithelial cells and decreases the motility of BC cells, thereby inhibiting tumor progression [29–32]. In our investigation, we observed an upregulation of TPM1 mRNA expression, accompanied by a reduction in the proliferation and migration of BC cells in the CYB561-shRNA group. Notably, TPM1 expression was discernible in single-cell analyses, and cells exhibiting this expression demonstrated notable similarities to CYB561 cells. Some studies have found an association between TPM1 and immune cell infiltration in tumors [33, 34]. Through sophisticated single-cell analysis, we found that macrophages in BC exhibited a distinct temporal developmental trajectory compared with other cell types. This differential trajectory signifies the unique functional and regulatory roles of macrophages in BC progression. Intriguingly, subsequent analysis of the biological functions of macrophages revealed their association with actin filament binding, suggesting a potential role for TPM1 in macrophage polarization. We hypothesized that CYB561 enhances BC cell proliferation, migration, and invasion by modulating TPM1 expression, potentially influencing M2 macrophage polarization. However, this hypothesis warrants further investigation.

We investigated the mechanistic role of CYB561 in BC using cellular experiments, single-cell analyses, and clinical cohorts. Despite these extensive efforts, our study has several limitations. First, as the study was retrospective in nature, it is potentially susceptible to selection bias. Second, it lacked a large multicenter sample, which would ensure more robust validation. Third, in our analysis of CYB561 function in BC, we initially focused on two TNBC cell lines selected based on their expression levels. Expanding the range of studied BC subtypes will enhance the scope of future investigations. Although our research has advanced the understanding of how CYB561 promotes BC progression, it unquestionably necessitates further empirical validation. Nonetheless, it has been established that CYB561 accelerates BC progression and is correlated with M2 macrophage polarization within the immune microenvironment, marking it as a potential therapeutic and prognostic target for BC.

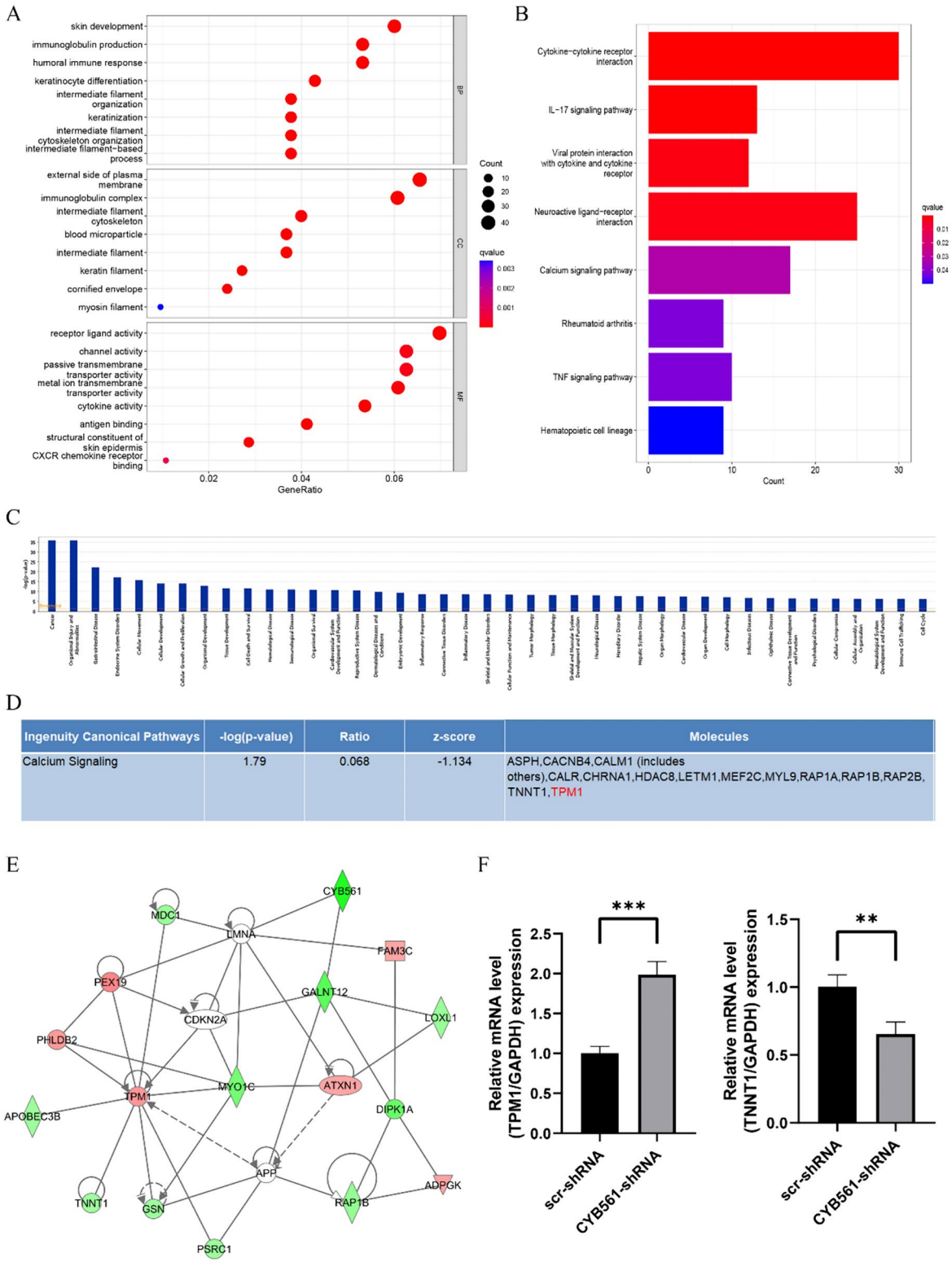

Fig. 7 CYB561-related signaling pathway analysis. **A** GO enrichment was performed to analyze the function of CYB561 in BC. **B** KEGG enrichment analysis of signaling pathways involved in CYB561 in BC. **C** IPA analyzes the relationship between CYB561 and disease. **D** IPA analysis of CYB561 in BC is associated with the calcium signaling pathway. **E** IPA constructs a reciprocal network between CYB561 and TPM1. **F** qRT-PCR was performed to detect the expression levels of TPM1, TNNT1 between the scr-shRNA and CYB561-shRNA groups

Conclusions

Elevated CYB561 expression suggests a poor prognosis for patients with BC and is associated with macrophage M2 polarization in the BC microenvironment. Therefore, CYB561 could potentially serve as a therapeutic target for BC treatment.

Abbreviations

ANOVA	Analysis of variance
AUC	Area under the receiver operating characteristic curve
BC	Breast cancer
CYB561	Cytochrome b561
FBS	Fetal bovine serum
FPKM	Fragments per kilobase of transcript per million mapped reads
GEO	Gene Expression Omnibus
GO	Gene Ontology
IHC	Immunohistochemistry
IPA	Innovative Pathway Analysis
KEGG	Kyoto Encyclopedia of Genes and Genomes
MTT	3-(4,5-Dimethylthiazol-2-yl)-2,5-diphenyltetrazolium bromide
OS	Overall survival
PBS	Phosphate-buffered saline
PCA	Principal component analysis
qRT-PCR	Quantitative real-time PCR
RFS	Recurrence-free survival
ROC	Receiver operating characteristic
ER	Estrogen receptor
PR	Progesterone receptor
HER2	Human epidermal growth factor receptor 2
scr	Scrambled
scRNA-seq	Single-cell RNA sequencing
shRNAs	Short hairpin RNAs
TCGA	The Cancer Genome Atlas
TNBC	Triple-negative breast cancer
TNMplot	Tumor–Normal–Metastatic Plot

Supplementary Information

The online version contains supplementary material available at https://doi.org/10.1186/s40001-024-02010-3.

Supplementary Material 1: Supplementary Fig. 1. Quality control of CYB561 single-cell analysis data. A. Screening of top 2000 variable genes based on GSE199515 dataset. B. The top 15 principal components were selected for further analysis. C. Reduced-dimensional class clustering of cells using UMAP. Supplementary Fig. 2. CYB561-related differential gene analysis. A. Based on the TCGA database, differential genes between high and low expression groups of CYB561 were analyzed. B. Based on gene chips, relevant differential genes were analyzed between the scr-shRNA group and the CYB561-shRNA group.

Acknowledgements

Not applicable.

Author contributions

JZ took part in the data curation, formal analysis, investigation and drafting the article. LD, AS and HY were involved in clinical resources. YZ, RH, HL, ZZ and YT were involved in methodology. RW and XY were responsible for methodology and project administration. WL made conceptualization, funding acquisition and final review of the manuscript. All authors read and approved the final manuscript.

Funding

This work was supported by the Research project special fund of Yangzhou Municipal Health and Health Committee (2023-2-13).

Availability of data and materials

The data that support the findings of this study are openly available on the TCGA database (https://portal.gdc.cancer.gov/) and the GEO database (https://www.ncbi.nlm.nih.gov/geo/).

Declarations

Ethics approval and consent to participate

This study was retrospective in nature and anonymization of all patient information would not have impacted the treatment and therefore approval was obtained from the Ethics Committee of Yangzhou Maternal and Child Health Care Hospital Affiliated to Yangzhou University to waive patient informed consent.

Consent for publication

Not applicable.

Competing of interests

The authors declare no competing interests.

Received: 17 February 2024 Accepted: 2 August 2024
Published online: 12 August 2024

References

1. Dastjerd NT, Valibeik A, Rahimi Monfared S, Goodarzi G, Moradi Sarabi M, Hajabdollahi F, et al. Gene therapy: a promising approach for breast cancer treatment. Cell Biochem Funct. 2022;40:28–48.
2. Sung H, Ferlay J, Siegel RL, Laversanne M, Soerjomataram I, Jemal A, et al. Global Cancer Statistics 2020: GLOBOCAN estimates of incidence and mortality worldwide for 36 cancers in 185 countries. CA Cancer J Clin. 2021;71:209–49.
3. Wen X-F, Chen M, Wu Y, Chen M-N, Glogowska A, Klonisch T, et al. Inhibitor of DNA binding 2 inhibits epithelial-mesenchymal transition via up-regulation of notch3 in breast cancer. Transl Oncol. 2018;11:1259–70.
4. Zhang X, Yang L, Chien S, Lv Y. Suspension state promotes metastasis of breast cancer cells by up-regulating cyclooxygenase-2. Theranostics. 2018;8:3722–36.
5. Denkert C, Loibl S. Response-based molecular subtyping—emergence of the third generation of breast cancer subtypes. Cancer Cell. 2022;40:592–4.
6. Asard H, Barbaro R, Trost P, Bérczi A. Cytochromes *b* 561: ascorbate-mediated trans-membrane electron transport. Antioxid Redox Signal. 2013;19:1026–35.
7. Bérczi A, Zimányi L. The trans-membrane cytochrome b561 proteins: structural information and biological function. Curr Protein Pept Sci. 2014;15:745–60.
8. Shibao CA, Garland EM, Black BK, Mathias CJ, Grant MB, Root AW, et al. Congenital absence of norepinephrine due to CYB561 mutations. Neurology. 2020;94:e200–4.
9. van den Berg MP, Almomani R, Biaggioni I, van Faassen M, van der Harst P, Silljé HHW, et al. Mutations in CYB561 causing a novel orthostatic hypotension syndrome. Circ Res. 2018;122:846–54.
10. Sun D, Zhang A, Gao B, Zou L, Huang H, Zhao X, et al. Identification of alternative splicing-related genes CYB561 and FOLH1 in the tumor-immune microenvironment for endometrial cancer based on TCGA data analysis. Front Genet. 2022;13: 770569.
11. Li L, Li Z, Qu J, Wei X, Suo F, Xu J, et al. Novel long non-coding RNA CYB561-5 promotes aerobic glycolysis and tumorigenesis by interacting with basigin in non-small cell lung cancer. J Cell Mol Med. 2022;26:1402–12.
12. Willis S, Villalobos VM, Gevaert O, Abramovitz M, Williams C, Sikic BI, et al. Single gene prognostic biomarkers in ovarian cancer: a meta-analysis. PLoS ONE. 2016;11:e0149183.
13. Yang X, Zhao Y, Shao Q, Jiang G. Cytochrome *b* 561 serves as a potential prognostic biomarker and target for breast cancer. Int J Gen Med. 2021;14:10447–64.

14. Zhou X, Shen G, Ren D, Guo X, Han J, Guo Q, et al. Expression and clinical prognostic value of CYB561 in breast cancer. J Cancer Res Clin Oncol. 2022;148:1879–92.
15. Clough E, Barrett T. The Gene Expression Omnibus Database. In: Davis S, Mathé E, editors. Stat Genomics. New York: Springer; 2016. p. 93–110. https://doi.org/10.1007/978-1-4939-3578-9_5.
16. Wu T, Hu E, Xu S, Chen M, Guo P, Dai Z, et al. clusterProfiler 4.0: a universal enrichment tool for interpreting omics data. The Innovation. 2021;2: 100141.
17. Kanehisa M, Furumichi M, Sato Y, Kawashima M, Ishiguro-Watanabe M. KEGG for taxonomy-based analysis of pathways and genomes. Nucleic Acids Res. 2023;51:D587–92.
18. Chen B, Khodadoust MS, Liu CL, Newman AM, Alizadeh AA. Profiling tumor infiltrating immune cells with CIBERSORT. In: Von Stechow L, editor. Cancer system: biology. New York: Springer New York; 2018. p. 243–59. https://doi.org/10.1007/978-1-4939-7493-1_12.
19. Dieci MV, Miglietta F, Guarneri V. Immune infiltrates in breast cancer: recent updates and clinical implications. Cells. 2021;10:223.
20. Wu K, Lin K, Li X, Yuan X, Xu P, Ni P, et al. Redefining tumor-associated macrophage subpopulations and functions in the tumor microenvironment. Front Immunol. 2020;11:1731.
21. Ni C, Yang L, Xu Q, Yuan H, Wang W, Xia W, et al. CD68- and CD163-positive tumor infiltrating macrophages in non-metastatic breast cancer: a retrospective study and meta-analysis. J Cancer. 2019;10:4463–72.
22. Choi J, Gyamfi J, Jang H, Seung J. The role of tumor-associated macrophage in breast cancer biology. Histol Histopathol. 2017;33:133–45.
23. Jeong H, Hwang I, Kang SH, Shin HC, Kwon SY. Tumor-associated macrophages as potential prognostic biomarkers of invasive breast cancer. J Breast Cancer. 2019;22:38.
24. Zhang H, Zhu Z, Modrak S, Little A. Tissue-resident memory CD4+ T cells play a dominant role in the initiation of antitumor immunity. J Immunol. 2022;208:2837–46.
25. Nelson MA, Ngamcherdtrakul W, Luoh S-W, Yantasee W. Prognostic and therapeutic role of tumor-infiltrating lymphocyte subtypes in breast cancer. Cancer Metastasis Rev. 2021;40:519–36.
26. Brown JH, Kim KH, Jun G, Greenfield NJ, Dominguez R, Volkmann N, et al. Deciphering the design of the tropomyosin molecule. Proc Natl Acad Sci USA. 2001;98:8496–501.
27. Perry SV. Vertebrate tropomyosin: distribution, properties and function. J Muscle Res Cell Motil. 2001;22:5–49.
28. Bharadwaj S, Prasad GL. Tropomyosin-1, a novel suppressor of cellular transformation is downregulated by promoter methylation in cancer cells. Cancer Lett. 2002;183:205–13.
29. Da Costa GG, Gomig THB, Kaviski R, Santos Sousa K, Kukolj C, De Lima RS, et al. Comparative proteomics of tumor and paired normal breast tissue highlights potential biomarkers in breast cancer. Cancer Genomics Proteomics. 2015;12:251–61.
30. Qi L, Bart J, Tan LP, Platteel I, van der Sluis T, Huitema S, et al. Expression of miR-21 and its targets (PTEN, PDCD4, TM1) in flat epithelial atypia of the breast in relation to ductal carcinoma in situ and invasive carcinoma. BMC Cancer. 2009;9:163.
31. Dube S, Thomas A, Abbott L, Benz P, Mitschow C, Dube DK, et al. Expression of tropomyosin 2 gene isoforms in human breast cancer cell lines. Oncol Rep. 2016;35:3143–50.
32. Li D-Q, Wang L, Fei F, Hou Y-F, Luo J-M, Wei-Chen, et al. Identification of breast cancer metastasis-associated proteins in an isogenic tumor metastasis model using two-dimensional gel electrophoresis and liquid chromatography-ion trap-mass spectrometry. Proteomics. 2006;6:3352–68.
33. Liu X, Li X, Kuang Q, Luo H. Screening of immunotherapy-related genes in bladder cancer based on GEO datasets. Front Oncol. 2023;13:1176637.
34. Yan Y, Li J, Ye M, Li Z, Li S. Tropomyosin is potential markers for the diagnosis and prognosis of bladder cancer. Dis Markers. 2022;2022:6936262.

Publisher's Note